Crystallization of Brownian particles in thin systems constrained by walls

Crystallization of Brownian particles in thin systems constrained by walls

Mamoru Fujine,[1] Masahide Sato,[2] Tetsuya Toyooka,[3] Hiroyasu Katsuno,[4] Yoshihisa Suzuki,[5] and Tsutomu Sawada[6]
[1]*Graduate School of Natural Science and Technology, Kanazawa University, Kakuma-machi, Kanazawa 920-1192, Japan*
[2]*Information Media Center, Kanazawa University, Kakuma-machi, Kanazawa 920-1192, Japan*
[3]*Graduate School of Advanced Technology and Science, The University of Tokushima, 2-1 Minamijosanjima, Tokushima 770-8506, Japan*
[4]*Faculty of Science and Engineering, Ritsumeikan University, Kusatsu, Shiga 525-8577, Japan*
[5]*Institute of Technology and Science, The University of Tokushima, 2-1, Minamijosanjima, Tokushima, Tokushima 770-8506, Japan*
[6]*National Institute for Materials Science, 1-1 Namiki, Tsukuba, Ibaraki 305-0044, Japan*
(Received 27 June 2014; revised manuscript received 19 August 2014; published 22 September 2014)

Keeping formation of a colloidal crystal by a centrifugal force in mind, we carry out Brownian dynamics simulations in thin systems and study ordering of particles induced by an external force. During solidification, the two-dimensional ordering along walls initially occurs. Then, the ordered particles on the walls act as substrates, and crystallization proceeds into bulk. When the external force is weak, the close-packed face of the crystal structure is parallel to the bottom wall. The direction of the close-packed face depends on the strength of the external force: The close-packed face becomes parallel to the side walls with a strong external force.

DOI: 10.1103/PhysRevE.90.032404 PACS number(s): 68.08.−p, 82.70.Dd, 82.60.Nh, 61.50.−f

I. INTRODUCTION

Colloidal crystals have possibilities to be used as materials for some devices. For example, close-packed colloidal crystals in which the lattice constant is as large as the diameter of submicron particles are considered to be the candidates of materials for photonic crystals. The close-packed colloidal crystals with the face centered cubic (fcc) structure are used as templates for inverse opals with a three-dimensional full photonic band gap [1] so that recently, much attention has been paid to the close-packed colloidal crystals. Sedimentation is one of the methods to create close-packed colloidal crystals [2–4]. Some groups used a patterned wall as a template in order to control the orientation of a growing interface and succeeded in forming large grains of colloidal crystals [2]. The method, which is called colloidal epitaxy, is an effective one to create high quality colloidal crystals but has some shortcomings. One of them is the expensiveness to create a large template. If the diameter of colloidal particles is changed, a template suitable for the particles is needed anew. In order to overcome the shortcomings, a regular array of square pyramidal pits [3] and a large square pyramidal pit [4] were used as substrates. When the angle of the pyramidal pits is suitable, irrespective of the diameter of colloidal particles [4], the $\{111\}$ faces of the fcc structure are formed along the walls of the pits. Since the $\{100\}$ face of the fcc structure is selected as the growing interface, the stacking way is unique. A square lattice is formed on the growing interface, and the formation of stacking faults is prevented. Indeed, the method may be easier than the colloidal epitaxy [2], but we may need some troublesome processes in order to create pyramidal pits precisely.

Recently, Suzuki *et al.* used a container with smooth walls and succeeded in creating large grains of colloidal crystal in a simple way [5]. One of the key points in their experiments is tilting the container. During centrifugal sedimentation, colloidal particles prefer to form a triangular lattice on the walls. Although a patterned wall or a pit is not used, the $\{100\}$ face of the fcc structure is selected as the growing interface by tilting the container with the suitable angle, and large grains of colloidal crystal are formed. In the experiment [5], processing of the walls of the container is not necessary so that the method is simpler and easier than that used in the experiments [2–4].

Keeping the experiment [5] in mind, we carried out Brownian dynamics simulations and studied how crystallization of particles with a short range repulsion proceeds under a uniform external force [6–9]. In our simulations, two-dimensional ordering of particles on walls occurred initially. The three-dimensional ordering was affected by the two-dimensional ordering on walls and spread in bulk. We controlled the direction of the external force and succeeded in forming large grains with the fcc structure. The results in our previous simulations [6–9] qualitatively agreed with the experiment [5], but the external forces were much stronger than those used in other studies [10–12]. Thus, in this paper, we set the external force in the direction perpendicular to the bottom walls and study how the process of ordering of particles is affected by the strength of the external force.

In Sec. II, we introduce our model, which is a simple standard one. In Sec. III, we introduce order parameters in order to determine the structure in bulk. In our simulation, we use a short range repulsion as the interaction between particles so that the fcc and hexagonal close-packed (hcp) structures are expected to be formed as close-packed structures. Thus, we introduce some order parameters in order to investigate the orientation order and judge the structure in bulk by the order parameters. In Sec. IV, we show the results of our simulations. In the experiment [5], the distance between two side walls is shorter, so we use a thin simulation box. In Sec. V, we summarize our results.

II. MODEL

We use a very simple model in our simulations. We neglect hydrodynamic effects and assume that the viscosity is high. The velocity of the ith particle is expressed as

$$\frac{d\boldsymbol{r}_i}{dt} = \frac{1}{\zeta}\left(F_{\rm ext}\mathbf{e}_{\rm ext} + \sum_{i\neq j}\boldsymbol{F}_{ij} + \boldsymbol{F}_i^{\rm B}\right), \tag{1}$$

where $\boldsymbol{r}_i$ is the position of the ith particle and ζ is the frictional coefficient. $F_{\rm ext}\mathbf{e}_{\rm ext}$ represents a uniform external force, where

$F_{\rm ext}$ and $\mathbf{e}_{\rm ext}$ are the strength and direction of the external force, respectively. When the interaction potential between the ith and the jth particles is given by $U(r_{ij})$, the force acting on the ith particle from the jth particle $\boldsymbol{F}_{ij}$ is expressed as $\boldsymbol{F}_{ij} = -\nabla U(r_{ij})$, where $r_{ij} = |\boldsymbol{r}_i - \boldsymbol{r}_j|$.

We assume that the interaction between particles is a short range repulsion. We use the Weeks-Chandler-Andersen (WCA) potential [13] defined as

$$U(r_{ij}) = \begin{cases} 4\epsilon\left[\left(\frac{\sigma}{r_{ij}}\right)^{12} - \left(\frac{\sigma}{r_{ij}}\right)^{6} + \frac{1}{4}\right], & (r \leqslant r_{\rm in}), \\ 0, & (r \geqslant r_{\rm in}), \end{cases} \quad (2)$$

where σ represents the diameter of particles and $r_{\rm in} = 2^{1/6}\sigma$. In Eq. (1), $\boldsymbol{F}_i^{\rm B}$ represents the random force, which satisfies the following relations:

$$\left\langle \boldsymbol{F}_i^{\rm B}(t) \right\rangle = \mathbf{0}, \quad (3)$$

$$\left\langle \boldsymbol{F}_i^{\rm B}(t) \cdot \boldsymbol{F}_j^{\rm B}(t') \right\rangle = 6\zeta k_{\rm B} T\, \delta_{ij}\delta(t - t'). \quad (4)$$

A simple normalized difference equation is given by [14]

$$\tilde{\boldsymbol{r}}_i(\tilde{t} + \Delta\tilde{t}) = \tilde{\boldsymbol{r}}_i(\tilde{t}) + \left(\tilde{F}_{\rm ext}\mathbf{e}_{\rm ext} + \sum_{i \neq j} \tilde{\boldsymbol{F}}_{ij} \right) \Delta\tilde{t} + \Delta\tilde{\boldsymbol{r}}_i^{\rm B}, \quad (5)$$

where the position, the distance, the time, and the forces are scaled as $\tilde{\boldsymbol{r}}_i = \boldsymbol{r}_i/\sigma$, $\tilde{t} = t\epsilon/\zeta\sigma^2$, $\tilde{F}_{\rm ext} = F_{\rm ext}\sigma/\epsilon$, and $\tilde{\boldsymbol{F}}_{ik} = \boldsymbol{F}_{ik}\sigma/\epsilon$. The normalized isotropic displacement by the random force $\Delta\tilde{\boldsymbol{r}}_i^{\rm B}$ satisfies

$$\left\langle \Delta\tilde{\boldsymbol{r}}_i^{\rm B}(t) \right\rangle = \mathbf{0}, \quad (6)$$

$$\left\langle \Delta\tilde{\boldsymbol{r}}_i^{\rm B}(t) \cdot \Delta\tilde{\boldsymbol{r}}_j^{\rm B}(t') \right\rangle = 6\tilde{R}^{\rm B}\Delta\tilde{t}\, \delta_{ij}\delta(t - t'), \quad (7)$$

where $\tilde{R}^{\rm B} = k_{\rm B}T/\epsilon$.

In Fig. 1 we show a typical shape of a simulation box and the initial positions of particles. Corners of the simulation box are named A, B, ..., F, and G (in Fig. 1, the corner E is hidden by particles). We use a periodic boundary condition in the y direction and consider walls in the x and z directions: The planes $ABCD$, $EFGH$, $CDGH$, and $BFEA$ are walls. Particles collide with the walls elastically. Since we add the external force whose x component is positive, the particles move toward the wall $ABCD$. Crystallization proceeds from the wall $ABCD$ to the right hand side so that we call the wall $ABCD$ the bottom wall. According to Ref. [5], walls $DCGH$ and $BFEA$ are called the upper side wall and the lower side wall, respectively.

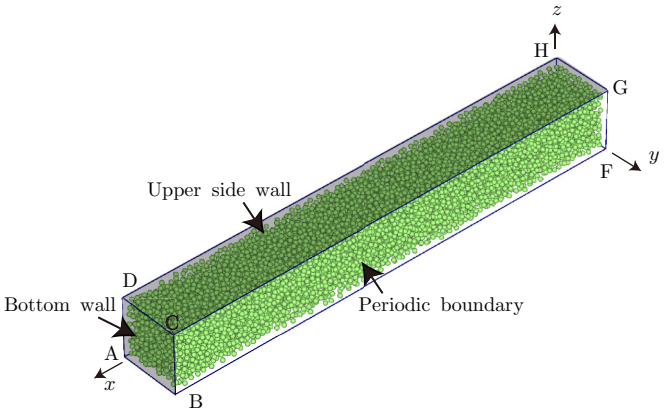

FIG. 1. (Color online) A typical shape of a container and the initial positions of particles.

III. ORDER PARAMETERS

In order to judge whether a particle is solidlike or liquidlike, we use an order parameter $d_l(i,j)$ [12,15]. Since we use the WCA potential, the distance between particles in bulk is about $r_{\rm in}$ if a close-packed structure is formed. However, the distance between particles is fluctuated by random displacements. Thus, we regard the jth particle as one of the neighbors of the ith particle when $|\boldsymbol{r}_{ij}|$ is smaller than $1.1r_{\rm in}$. When the jth particle is one of the neighbors of the ith particle, $d_l(i,j)$ is given by

$$d_l(i,j) = \sum_{m=-l}^{l} q_{l,m}(i) q_{l,m}^*(j), \quad (8)$$

where

$$q_{l,m}(i) = \frac{1}{n_{\rm n}} \sum_{j=1}^{n_{\rm n}} Y_l^m(\theta_{ij}, \phi_{ij}), \quad (9)$$

and $q_{l,m}^*(j)$ is the complex conjugate of $q_{l,m}(j)$. The angles θ_{ij} and ϕ_{ij} represent the polar and azimuthal angles, respectively. $Y_l^m(\theta_{ij}, \phi_{ij})$ is the spherical harmonics, and $n_{\rm n}$ is the number of neighboring particles.

Since particles are strongly pressed by a uniform external force, the hcp and fcc structures are expected to be formed in bulk in order to increase the density. We introduce parameters, $Q_l(i)$ and $w_l(i)$ [16–20] and determine the local structure. The definitions of $Q_l(i)$ and $w_l(i)$ are given by

$$Q_l(i) = \sqrt{\frac{4\pi}{(2l+1)} \sum_{m=-l}^{l} |q_{l,m}(i)|^2}, \quad (10)$$

$$w_l(i) = \frac{1}{g_l^{3/2}} \sum_{m_1+m_2+m_3=0} \begin{pmatrix} l & l & l \\ m_1 & m_2 & m_3 \end{pmatrix} \times q_{l,m_1}(i) q_{l,m_2}(i) q_{l,m_3}(i), \quad (11)$$

where g_l is defined as $g_l = \sum_{m=-l}^{l} |q_{l,m}(i)|^2$. The integers m_1, m_2, and m_3 run from $-l$ to l while satisfying the condition $m_1 + m_2 + m_3 = 0$, and the term in parentheses in Eq. (11) is the Wigner $3-j$ symbol [21].

Using $Q(l)$ and $w(l)$, we classify particles into five types of particles, i.e., dilute liquidlike particles, dense liquidlike particles, disordered solidlike particles, the hcp structured particles, and the fcc structured particles. Particles are regarded as the dilute liquidlike particles if the number of their neighbors is four or less. If the number of their neighbors is five or more, we use d_6 and judge whether the particles are solidlike particles or dense liquidlike particles. The particles are dense liquidlike particles when the number of connections between neighbors in which the parameter $d_6 > 0.7$ is four or less. If the number is five or more, we regard the particles as solidlike particles. Using $w_4(i)$ and $Q_4(i)$, we determine the structure of the solidlike particles which have 12 neighbors. Taking account of our previous studies [6–8], we regard the

particles as fcc structured particles if $-0.18 < w_4(i) < -0.01$ and $0.175 < Q_4(i) < 0.2$ and as hcp structured particles if $0.02 < w_4(i) < 0.15$ and $0.06 < Q_4(i) < 0.15$.

We consider walls in the x and z directions so that the close-packed faces of the hcp and fcc structures, which have the sixfold orientation symmetry, prefer to be parallel to the walls. In order to investigate the local sixfold orientation symmetry, we use the following order parameter [22–24]:

$$\psi(k) = \frac{1}{n(k)} \left| \sum e^{6i\theta_{km}} \right|, \tag{12}$$

where $n(k)$ represents the number of neighbors of the kth particle in the plane we focus on. If we investigate the sixfold orientation symmetry in the plane normal to the z axis, we see the particles whose z coordinate is the same as that of the kth particle (see Ref. [25]). When the difference in the z coordinates of the kth and mth particles $|z_k - z_m|$ is smaller than $\delta z = 0.1$, we consider that the mth and kth particles are in the same plane. θ_{km} is the angle between the vector $\boldsymbol{r}_{km} - (\boldsymbol{e}_z \cdot \boldsymbol{r}_{km})\boldsymbol{e}_z$ and the positive x direction, where $\boldsymbol{e}_z$ is the unit vector in the z direction. In our simulation, we regard the kth particle as the particle in the close-packed face parallel to the xy plane. We also carry out a similar calculation for the plane normal to the x axis.

IV. RESULTS

In our simulation, the scaled system size is $\tilde{L}_x \times \tilde{L}_y \times \tilde{L}_z = 8\tilde{L} \times \tilde{L} \times \tilde{L}$ with $\tilde{L} = 13.38$. The number of particles N is 10 976 so that the volume fraction of particles $4\pi N(\sigma/2)^3/(3L_xL_yL_z) = \pi N/(6\tilde{L}_x\tilde{L}_y\tilde{L}_z)$ is 0.3. The time increment $\Delta\tilde{t}$ is equal to or smaller than 10^{-4}, and the random displacement $\tilde{R}^B$ is 0.1.

In Fig. 2, we show snapshots in a late stage of solidification where we change the colors of the particles in order to distinguish the states of the particles. The dilute liquidlike particles, the dense liquidlike particles, the disordered solidlike particles, the hcp structured particles, and the fcc structured particles are colored white (the lightest), yellow (the second lightest), red (the darkest), orange (the second darkest), and blue (the third darkest), respectively. In Fig. 2(a), the external force is given by 0.2(1,0,0). In the solid phase, the hcp structured particles are more numerous than the fcc structured particles. Only a few particles with the fcc structure are formed near the solid-liquid interface. The close-packed face of the hcp structure is mainly parallel to the bottom wall. In

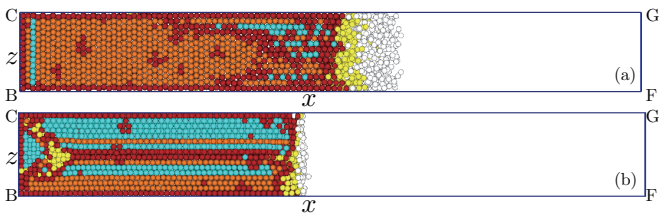

FIG. 2. (Color online) Snapshots of particle positions during solidification with (a) the external force 0.2(1,0,0) and (b) (1,0,0). The snapshots show the systems seen from the positive y direction. The scaled time $\tilde{t}$ is (a) 1000 and (b) 160, respectively.

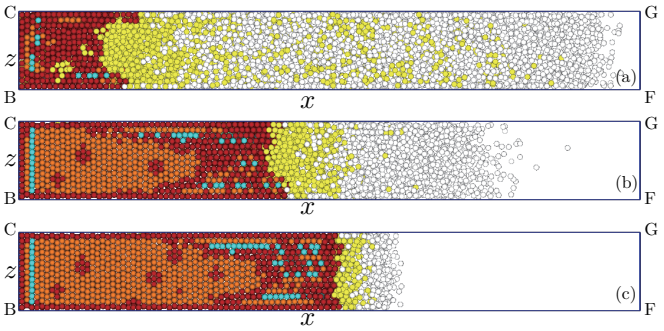

FIG. 3. (Color online) Snapshots of particle positions during solidification in a weak external force. The parameters are the same as those in Fig. 2(a). The scaled time $\tilde{t}$ is (a) 70, (b) 200, and (c) 900, respectively.

Fig. 2(b), the external force is (1,0,0), which is five times larger than that in Fig. 2(a). The number of liquidlike particles on the right hand side of the solid-liquid interface is smaller than that in Fig. 2(a). Both the hcp structure and the fcc structure are formed in the solid, and the close-packed faces of almost all of the ordered solid are parallel to the side wall, which are quite different from the features shown in Fig. 2(a). The structure in the solid is affected by the strength of the external force.

In Fig. 3, we show how the hcp structure is formed in bulk with a weak force. In an early stage [Fig. 3(a)], the solidlike structure is formed near the bottom wall. Only a few particles with the hcp and fcc structures appear in the solidlike structure. The number of the hcp structured particles is as large as that of the fcc structured particles. In the middle stage [(Fig. 3(b)], the hcp structure whose close-packed face is parallel to the bottom wall grows. Near the upper side wall, we can also see the hcp structure whose close-packed face is parallel to the wall. The position of the hcp structure shifts to the right hand side during growth, and the hcp structure with the close-packed face parallel to the side wall appears near the solid-liquid interface in a late stage [(Fig. 3(c)].

We see the change in the two-dimensional structure of particles attaching to the upper side wall during solidification. In Fig. 4, we show the snapshots seen from the positive z direction. When the distance between the upper wall and a particle is larger than 0.6, the particle is not regarded as attaching to the upper wall and is colored green (the second darkest). The colors of the particles attaching to the upper wall are the same as those in Fig. 2. In an early stage [Fig. 4(a)], the particles attaching to the upper wall form a triangular lattice. In a middle stage [Fig. 4(b)], the triangular lattice, whose side line is parallel to the y axis, is changed to the $(10\bar{1}0)$ face of the hcp structure when the hcp structure is formed in bulk. With increasing the hcp structure in bulk, the transition proceeds, and the two-dimensional structure spreads to the right hand side [Fig. 4(c)].

In our simulation the system size is narrow so that we doubt that the system size accidentally commensurates with the particle size. The hcp structure with the close-packed face parallel to the bottom wall happens to be formed in bulk. If we use a different system size, the structure in bulk may be drastically changed. In order to confirm the possibility, we carry out simulations in two simulation boxes with different

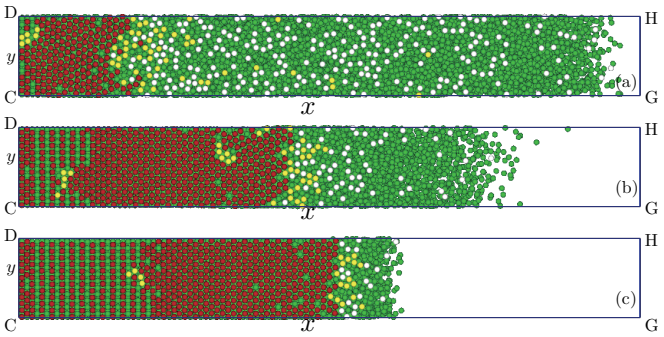

FIG. 4. (Color online) Snapshots of particle positions during solidification in a weak external force. The parameters are the same as those in Fig. 2(a). The snapshots show the systems seen from the positive z direction (the upper side wall). The scaled time $\tilde{t}$ is (a) 70, (b) 200, and (c) 900, respectively. The colors of the particles attaching to the wall are the same as those in Fig. 2(a). The particles not attaching to the upper wall are colored green (the second darkest) and are distinguished from the solidlike particles on walls colored red (the darkest).

L_z's. In Fig. 5, we show snapshots with two systems.L_x and L_y are same as those in Fig. 2. Since the effect of the distance between two side walls probably increases in a narrow system, we use L_z smaller than that in Fig. 2: $L_z = 3L/4$ in Fig. 5(a) and $L_z = 3L/4 + \sigma/2$ in Fig. 5(b). The external force is $F_{\rm ext} = 0.12$, which is smaller than that in Fig. 2(a). Both in Fig. 5(a) and in Fig. 5(b), the hcp structure whose close-packed face is parallel to the bottom wall is formed as in Fig. 2(a). The commensurability of the system size may be important if the system size is much narrower than in our systems, but the effect of the commensurability is not so large in our simulations.

We focus on the effect of $F_{\rm ext}$ on the structure in bulk. In Fig. 6 we show the time evolution of the numbers of the ordered particles.$N_{\rm s}$ is the number of particles whose close-packed face is parallel to the side wall, and $N_{\rm b}$ is that with the close-packed face parallel to the bottom wall. Using the parameter $\psi(k)$, we count the numbers of ordered particles $N_{\rm s}$ and $N_{\rm b}$. In an early stage, both $N_{\rm s}$ and $N_{\rm b}$ increase monotonically and saturate in a late stage.

When the force is weak [Fig. 6(a)], $N_{\rm b}$ is larger than $N_{\rm s}$. With a large $F_{\rm ext}$ [Fig. 6(b)], the saturation of $N_{\rm s}$ and $N_{\rm b}$ occurs fast, and the relation between $N_{\rm b}$ and $N_{\rm s}$ becomes the opposite to Fig. 6(a). Although the sum of $N_{\rm s}$ and $N_{\rm b}$, which represents

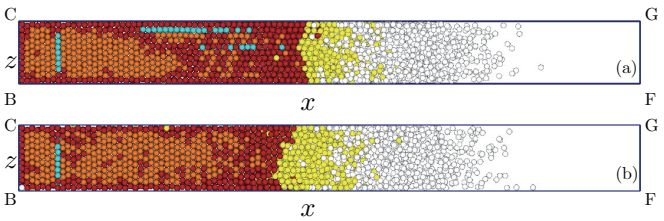

FIG. 5. (Color online) Snapshots in bulk with two systems. In the systems, $\tilde{L}_x = 8\tilde{L}$ and $\tilde{L}_y = \tilde{L}$, which are the same as those in Fig. 2. $\tilde{L}_z$ is (a) $3\tilde{L}/4$ and (b) $3\tilde{L}/4 + \sigma/2$. The number of particles is $3N/4$. The external force is $F_{\rm ext} = 0.12$. $\Delta\tilde{t} = 8.0 \times 10^{-4}$ and $\tilde{t} = 400$.

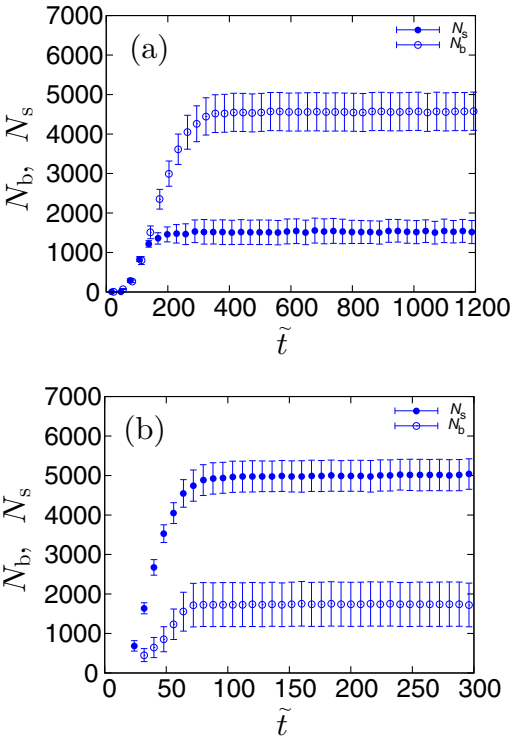

FIG. 6. (Color online) Time evolution of the numbers of ordered particles. $N_{\rm s}$ and $N_{\rm b}$ represent the numbers of ordered particles whose close-packed face is parallel to the side wall and the bottom wall, respectively. The data are averaged over ten runs. The strength of the external force is (a) 0.2 and (b) 1.0.

the number of all the ordered particles, is hardly changed by $F_{\rm ext}$, the direction of the close-packed face is strongly influenced by $F_{\rm ext}$. Figure 7 represents the dependence of the saturated values of $N_{\rm b}$ and $N_{\rm s}$ on $F_{\rm ext}$.$N_{\rm b}$ is larger than $N_{\rm s}$ when $F_{\rm ext}$ is small. The bottom wall affects the ordering of particles stronger than the side walls. With increasing $F_{\rm ext}$, $N_{\rm b}$ deceases rapidly and $N_{\rm s}$ increases. When $F_{\rm ext}$ is 0.3, the number $N_{\rm s}$ is larger than $N_{\rm b}$. We find that the effect of the side walls on the ordering of particles becomes large with increasing $F_{\rm ext}$.

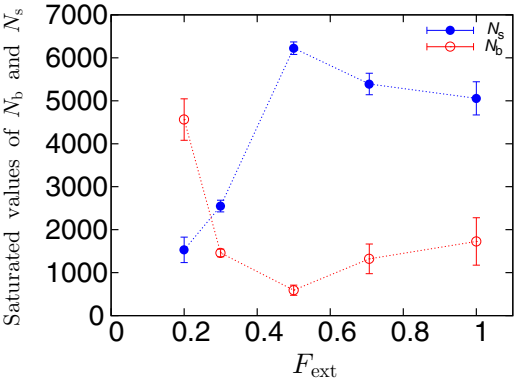

FIG. 7. (Color online) Dependence of the saturated values of $N_{\rm b}$ and $N_{\rm s}$ on the strength of external force. The data are averaged over ten runs.

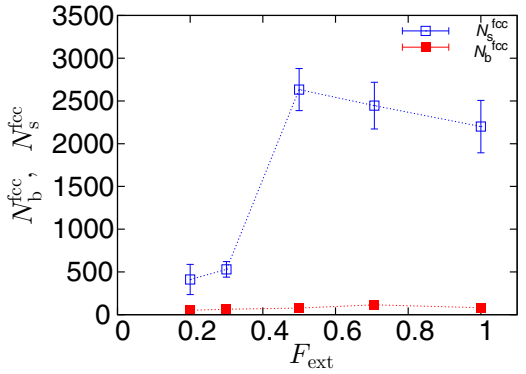

FIG. 8. (Color online) Dependence of the saturated number of fcc structured particles on the strength of external force. N_s^{fcc} and N_b^{fcc} represent the saturated number of the fcc structured particles whose close-packed face is parallel to the side wall and the bottom wall, respectively. The data are averaged over ten runs.

In Fig. 8, we show how the saturated number of the fcc structured particles depends on the strength of the external force F_{ext}.N_s^{fcc} and N_b^{fcc} represent the saturated number of the fcc structured particles whose close-packed face is parallel to the side wall and the bottom wall, respectively. The fcc structured particles affected by the bottom wall are hardly formed irrespective of F_{ext}. On the other hand, N_s^{fcc} suddenly becomes large when $F_{ext} \geqslant 0.3$. From Figs. 7 and 8, we find that the increase in the saturated value of N_s in Fig. 7 is mainly caused by the change in N_s^{fcc}.

A. Comparison with an experiment

We compare the results of our simulation with an experiment with spherical polystyrene particles (Duke Scientific Co. Ltd., 5020A, diameter of particles is about 200 nm) in water. The container was made of a cycloolefin copolymer (Mitsui Chemicals, Inc., APL5014DP), and its inner size was $L_x \times L_y \times L_z = 50.0 \times 8.0 \times 0.1$ mm^3.

After the suspensions of particles were injected into containers and bubbles inside were removed completely by applying centrifugation, we carried out the experiment. The container was set horizontally on a centrifugal apparatus [5] and was rotated. Using two centrifugal forces we investigated how the influence of the side walls changes with the strength of the force.

In Fig. 9 we show typical merged reflection bright-field images. The region in which the close-packed face is parallel to the upper side wall is colored green (light). With a strong force [Fig. 9(a)], the green region spreads over the whole container. On the other hand, the ratio of the green region decreases with the weak force [Fig. 9(b)]. In Ref. [26], Hashimoto *et al.* carried out an experiment with a weaker centrifugal force and showed that the bottom wall affects the grain formation strongly. Thus, we guess that the close-packed face is parallel to the bottom wall in the dark region. Since the region seems to increase with decreasing the strength of the centrifugal force, the dependence of the orientation of the close-packed face on the external force in our simulation qualitatively agrees with the experiment.

In our model, we assumed that $m\ddot{\boldsymbol{x}} \ll \zeta\dot{\boldsymbol{x}}$ and neglected the acceleration term. The assumption is valid when $\tau = m/\zeta$ is

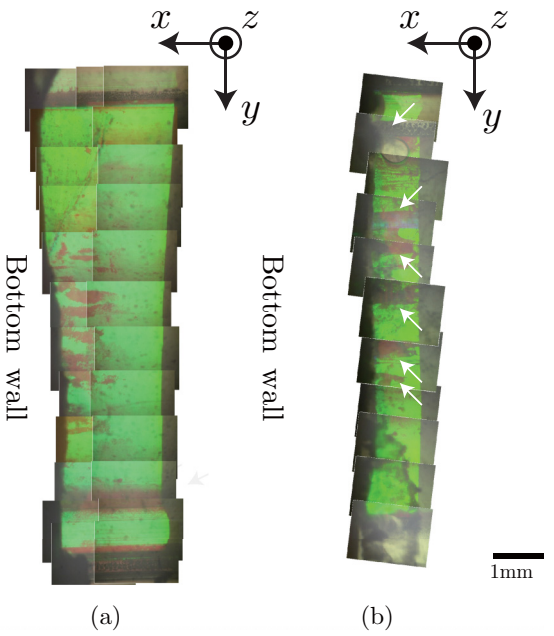

FIG. 9. (Color online) Typical merged reflection bright-field images, which are viewed from the upper side direction similar to Fig. 4. Black arrows show the direction of the axes. White arrows in (b) show the region in which the close-packed face is not parallel to the side wall. The strength of the centrifugal force is (a) $336g$ and (b) $42g$, where g represents the gravitational acceleration rate. The time interval in which the centrifugal force is added is about (a) 19 h 10 min and (b) 39 h 50 min. The length scale of a black bar at the right bottom is about 1 mm.

much smaller than $\zeta\sigma/F_{ext}$. In our experiment, the diameter of particles σ is about 200 nm, and the coefficient of viscosity of water η in room temperature is about 0.010 g/cm^3 so that the friction coefficient $\zeta = 3\pi a\eta$ is estimated to be 1.88×10^{-6} g/s. The mass of a particle m is 4.40×10^{-15} g. Thus, the relaxation time τ is estimated as $\tau = 2.34 \times 10^{-9}$ s. Another characteristic time $\zeta\sigma/F_{ext}$ is about 2.6×10^{-2} s to 2.1×10^{-1} s. Thus, since τ is much smaller than $\zeta\sigma/F_{ext}$, the relaxation to the terminal velocity occurs very fast. We could not help using a large external force in our simulations [6,7] because of the restriction of the computational resource, but our assumption of neglecting the acceleration term is valid in order to explain the motion of particles in our experiment. We also estimate the Peclet number (Pe) defined as $m_B a\sigma/k_B T$, where m_B is the buoyant mass of a particle and a is the acceleration rate. The Pe is estimated to be 1.7×10^{-2} in Fig. 9(a) and 2.0×10^{-3} in Fig. 9(b). In our simulation, the Pe is 0.6 when the external force is $\tilde{F}_{ext} = 0.12$. The external forces we used in this paper are smaller than those in our previous studies, but they are larger than that in our experiment. Thus, we need to note the difference in the Peclet number when we try to compare the simulations with the experiment quantitatively.

B. Comparison with results in a system with periodic boundaries

When the external force is small, the main structure formed in bulk is the hcp structure in Fig. 2. However, the formation

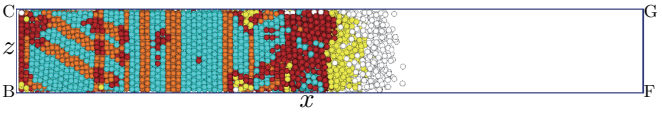

FIG. 10. (Color online) Snapshots of particles in the system without side walls. The time $\tilde{t} = 1000.0$. Parameters are the same as those in Fig. 2(a).

of large grains with the fcc structure has been reported in experiments [2,3]. In our simulation, the distance between the side walls is much smaller so that the effect of the constraint by the side walls is large. The difference in the structure between the experiments [2,3] and our simulation is probably caused by the effect of the side walls. In order to confirm the effect of the side walls, we carry out a simulation without the side walls. In Fig. 10 we show a typical snapshot of the system without the side walls. Except for the boundary condition, the parameters are the same as those in Fig. 2(a). The close-packed face is parallel to the bottom wall, which is similar to the results in the system with the side walls. However, the structure of the ordered particles is mainly the fcc structure, which is markedly differently from Fig. 2 and agrees with the experiments [2,3].

Figure 11 shows the time evolution of the ratio of the number of the fcc ordered particles N^{fcc} to that of all ordered particles N_{ordered} with $F_{\mathrm{ext}} = 0.2$. In the initial stage, the ratio of $N^{\mathrm{fcc}}/N_{\mathrm{ordered}}$ in the system with the side walls is roughly as large as that in the system without the side walls. The ratio decreases with increasing time when the side walls are present. On the other hand, the ratio in the system without the side walls increases.

Figure 12 shows the dependence of the saturated value of $N^{\mathrm{fcc}}/N_{\mathrm{ordered}}$ on F_{ext}. When the side walls are absent, the saturated ratio $N^{\mathrm{fcc}}/N_{\mathrm{ordered}}$ hardly changes and is kept about 0.6. In the system with the side walls, the ratio $N^{\mathrm{fcc}}/N_{\mathrm{ordered}}$ is smaller than that in the system without the side walls. When $\tilde{F}_{\mathrm{ext}}$ is large, the ratio $N^{\mathrm{fcc}}/N_{\mathrm{ordered}}$ is about 0.4. When $\tilde{F}_{\mathrm{ext}} \leqslant 0.5$, the ratio becomes small with decreasing $\tilde{F}_{\mathrm{ext}}$.

From Figs. 2(a) and 10–12, we confirmed that side walls play an important role for the structure in bulk. We think

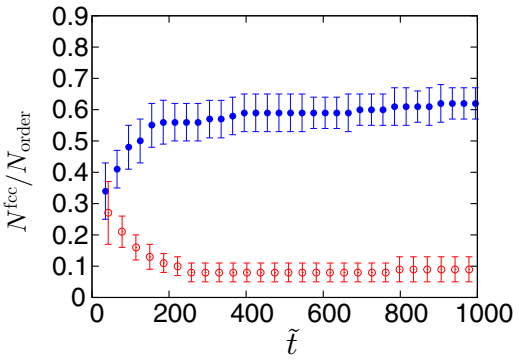

FIG. 11. (Color online) Time evolution of the ratio of the number of the fcc ordered particles N^{fcc} to that of all ordered particles N_{ordered}. Open circles and solid circles show the data with and without walls, respectively. Parameters are the same as those in Fig. 2(a).

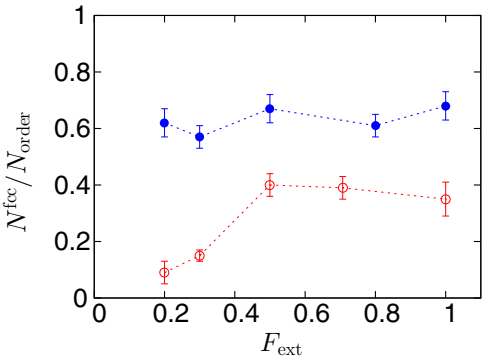

FIG. 12. (Color online) Dependence of the saturated value of $N^{\mathrm{fcc}}/N_{\mathrm{ordered}}$ on F_{ext} in a system. Open circles and solid circles show the data with and without walls, respectively. The data are averaged over ten samples.

that the formation of the hcp structure in Fig. 2(a) may be explained by the two-dimensional structure on the side walls. In Fig. 4, the particles attaching to the side walls initially form a triangular lattice. One of the side lines of the lattice is roughly parallel to the edge CD. With the formation of the hcp structure in bulk, the lattice structure is changed to the $(10\bar{1}0)$ face of the hcp structure. If the fcc structure is formed in bulk and the (111) face is formed on the bottom wall, the $(11\bar{2})$ face of the fcc structure is necessary to be formed on the top side wall. Considering the symmetry of the $(10\bar{1}0)$ face of the hcp structure and the $(11\bar{2})$ face of the fcc structure, transition from the triangular lattice to the $(10\bar{1}0)$ face of the hcp structure seems to be easier than that to the $(11\bar{2})$ face of the fcc structure. In addition, when the density of particles becomes high and particles are strongly pressed on walls, the $(11\bar{2})$ face probably becomes unstable. Thus, the hcp structure is probably formed in the system with the side walls.

V. SUMMARY

In this paper, keeping the formation of a colloidal crystal by centrifugal force in mind, we studied the ordering of particles in thin systems constrained by walls. We fixed the direction of the force to be parallel to the bottom wall and carried out simulations. When the external force was weak, the close-packed face was parallel to the bottom wall, and the hcp structure was mainly formed. With increasing the strength of the external force, the direction of the close-packed face is changed. The close-packed face parallel to the side walls became dominant, and both the fcc structure and the hcp structure coexisted. The external forces in our simulations were much larger than centrifugal forces in experiments, but the tendency obtained in simulation was also observed in our experiment as shown in Fig. 9.

We also carried out a simulation in the system without the side walls. In the system, the fcc structure was mainly formed with a weak force, which is quite different from the formation of the hcp structure in the system with walls. Thus, we found the side walls affect the type of solid structure in the thin system.

ACKNOWLEDGMENTS

This work was supported by Grants-in-Aids for Scientific Research on Innovative Areas "Fluctuation & Structure" (Grant No. 26103515) and Scientific Research (C) (Grant No. 26390054) from the Japan Society for the Promotion of Science, and some parts of this study were carried out under the Joint Research Program of the Institute of Low Temperature Science, Hokkaido University.

[1] A. Blanco, E. Chomski, S. Grabtchak, M. Ibisate, S. John, S. W. Leonard, C. Lopez, F. Meseguer, H. Miguez, J. P. Mondia, G. A. Ozin, O. Toader, and H. M. Van Diel, Nature (London) **405**, 437 (2000).
[2] A. V. Blaaderen, R. Ruel, and P. Wiltzius, Nature (London) **385**, 321 (1997).
[3] Y. Yin and Z. Li, and Y. Xia, Langmuir **19**, 622 (2003).
[4] S. Matsuo, T. Fujine, K. Fukuda, S. Joudokazis, and H. Misawa, Appl. Phys. Lett. **82**, 4283 (2003).
[5] Y. Suzuki, A. Mori, M. Sato, H. Katsuno, and T. Sawada, J. Cryst. Growth **401**, 905 (2014).
[6] M. Sato, H. Katsuno, and Y. Suzuki, Phys. Rev. E **87**, 032403 (2013).
[7] M. Sato, H. Katsuno, and Y. Suzuki, J. Phys. Soc. Jpn. **82**, 084804 (2013).
[8] M. Sato, H. Katsuno, and Y. Suzuki, J. Cryst. Growth **401**, 87 (2014).
[9] M. Fujine, M. Sato, H. Katsuno, and Y. Suzuki, Phys. Rev. E **89**, 042401 (2014).
[10] H. Mìguez, F. Meseguer, C. López, A. Misfud, J. S. Moya, and L. Vázquez, Langmuir **13**, 6009 (1997).
[11] P. Hoogenboom, D. Derks, P. Vergeer, and A. van Blaaderen, J. Chem. Phys. **117**, 11320 (2002).
[12] M. Marechal, M. Hermes, and M. Dijkstra, J. Chem. Phys. **135**, 034510 (2011).
[13] J. D. Weeks, D. Chandler, and H. C. Andersen, J. Chem. Phys. **54**, 5237 (1971).
[14] D. L. Ermak, J. Chem. Phys. **62**, 4189 (1975).
[15] P. R. ten Wolde, M. J. Ruiz-Montero, and D. Frenkel, Phys. Rev. Lett. **75**, 2714 (1995).
[16] P. J. Steinhardt, D. R. Nelson, and M. Ronchetti, Phys. Rev. B **28**, 784 (1983).
[17] M. D. Rintoul and S. Torquato, J. Chem. Phys. **105**, 9258 (1996).
[18] W. Lechner and C. Dellago, J. Chem. Phys. **129**, 114707 (2008).
[19] A. Panaitescu, K. A. Reddy, and A. Kudrolli, Phys. Rev. Lett. **108**, 108001 (2012).
[20] C. Desgranges and J. Delhommelle, Phys. Rev. B **77**, 054201 (2008).
[21] L. Landau and E. Lifschitz, *Quantum Mechanics* (Pergamon, London, 1965).
[22] R. Yamamoto and A. Onuki, J. Phys. Soc. Jpn. **66**, 2545 (1997).
[23] R. Yamamoto and A. Onuki, Phys. Rev. E **58**, 3515 (1998).
[24] T. Hamanaka and A. Onuki, Phys. Rev. E **74**, 011506 (2006).
[25] H. Tanaka and T. Araki, Phys. Rev. Lett. **85**, 1338 (2000).
[26] K. Hashimoto, A. Mori, K. Tamura, and Y. Suzuki, Jpn. J. Appl. Phys. **52**, 030201 (2013).